2-23-2022

Lipidomics analysis of outer membrane vesicles and elucidation of the inositol phosphoceramide biosynthetic pathway in Bacteroides thetaiotaomicron

Mariana G Sartorio

Ezequiel Valguarnera

Fong-Fu Hsu

Mario F Feldman

AMERICAN SOCIETY FOR MICROBIOLOGY | Microbiology Spectrum

RESEARCH ARTICLE

Lipidomics Analysis of Outer Membrane Vesicles and Elucidation of the Inositol Phosphoceramide Biosynthetic Pathway in *Bacteroides thetaiotaomicron*

Mariana G. Sartorio,[a] Ezequiel Valguarnera,[a]* Fong-Fu Hsu,[b] Mario F. Feldman[a]

[a]Department of Molecular Microbiology, Washington University School of Medicine, St. Louis, Missouri, United States
[b]Division of Endocrinology, Metabolism and Lipid Research, Washington University School of Medicine, St. Louis, Missouri, United States

Mariana G. Sartorio and Ezequiel Valguarnera contributed equally to this article. Author order was defined alphabetically.

ABSTRACT Approximately one-third of the human colonic microbiome is formed by bacteria from the genus *Bacteroides*. These bacteria produce a large amount of uniformly sized outer membrane vesicles (OMVs), which are equipped with hydrolytic enzymes that play a role in the degradation of diet- and host-derived glycans. In this work, we characterize the lipid composition of membranes and OMVs from *Bacteroides thetaiotaomicron* VPI-5482. Liquid chromatography-mass spectrometry (LC-MS) analysis indicated that OMVs carry sphingolipids, glycerophospholipids, and serine-dipeptide lipids. Sphingolipid species represent more than 50% of the total lipid content of OMVs. The most abundant sphingolipids in OMVs are ethanolamine phosphoceramide (EPC) and inositol phosphoceramide (IPC). Bioinformatics analysis allowed the identification of the *BT1522–1526* operon putatively involved in IPC synthesis. Mutagenesis studies revealed that *BT1522–1526* is essential for the synthesis of phosphatidylinositol (PI) and IPC, confirming the role of this operon in the biosynthesis of IPC. *BT1522–1526* mutant strains lacking IPC produced OMVs that were indistinguishable from the wild-type strain, indicating that IPC sphingolipid species are not involved in OMV biogenesis. Given the known role of sphingolipids in immunomodulation, we suggest that OMVs may act as long-distance vehicles for the delivery of sphingolipids in the human gut.

IMPORTANCE Sphingolipids are essential membrane lipid components found in eukaryotes that are also involved in cell signaling processes. Although rare in bacteria, sphingolipids are produced by members of the phylum Bacteroidetes, human gut commensals. Here, we determined that OMVs carry sphingolipids and other lipids of known signaling function. Our results demonstrate that the *BT1522–1526* operon is required for IPC biosynthesis in *B. thetaiotaomicron*.

KEYWORDS *Bacteroides*, OMV, ceramide, sphingolipids

From birth, the mammalian gastrointestinal tract is colonized by tens of trillions of microorganisms (1, 2). The sum of all microbes within an organism, or the microbiome, has been found to be key for the development of the host immune system (3–7). Increasing evidence suggests that alterations in the mammalian colonic microbiome can influence host health and disease outcomes (8–11). Moreover, gut disease in humans has been associated with altered microbial metabolic pathways (12, 13). Approximately one-third of the human colonic microbiome is formed by bacteria from the genus *Bacteroides*, which specializes in the degradation of complex dietary polysaccharides (1, 2, 14). *Bacteroides thetaiotaomicron*, a common human gut commensal, has been recognized as both beneficial and detrimental to the host, according to

Editor Silvia Bulgheresi, University of Vienna

Address correspondence to Mario F. Feldman, mariofeldman@wustl.edu.

*Present address: Ezequiel Valguarnera, Division of Critical Care Medicine, Department of Pediatrics, Washington University School of Medicine, St. Louis, Missouri, United States.

The authors declare no conflict of interest.

Received 21 June 2021
Accepted 19 December 2021
Published 26 January 2022

different murine models of inflammatory disease (15–17). Components of the *Bacteroides* cell envelope, such as the capsule, proteins with hydrolytic activity, and outer membrane vesicles (OMVs), have been implicated in shaping host-symbiont interactions (17–19).

Our group has shown that a subset of proteins from *Bacteroides* spp. predicted to localize to the outer membrane (OM) are preferentially enriched in OMVs (20–22). OMVs are spherical outer membrane-derived structures that contain outer membrane and periplasmic proteins, lipids, and other molecules such as lipopolysaccharides and capsules (23–25). The proteins enriched in OMVs are mainly lipoproteins with either glycosidase or protease activity that play a role in the digestion of complex nutrients. The intrinsic properties of these proteins, such as their isoelectric points and the presence of lipoprotein export signals (LES), account for their enrichment into OMVs (21, 22). However, while *Bacteroides* OMV cargo proteins have been well described, the lipid composition of OMVs and the effect of lipids on OMV biogenesis and cargo selection remain elusive.

Although rare in bacteria, sphingolipids are produced by members of the phyla Bacteroidetes and Proteobacteria (26–29). Sphingolipids are ubiquitous and structurally diverse polar lipids, essential for eukaryotic cell membrane homeostasis (30). Different sphingolipids have been linked to a plethora of cell signaling processes, including cell death, proliferation, growth, and migration (31). These bioactive molecules have also been shown to play important roles in the development of metabolic disorders, including the ability to interfere with cholesterol absorption and insulin resistance (32–34). Furthermore, microbially derived membrane sphingolipids have been linked to reduced inflammatory disease in humans and germfree mouse models (35, 36). Species from the phylum Bacteroidetes, including the human commensals *Bacteroides* and *Porphyromonas*, synthesize sphingolipids as the main constituents of their membranes (26, 35, 37–41). Despite the knowledge that members of the human microbiota produce eukaryotic-like lipids that are associated with health and disease states, there has been a paucity of mechanistic insights into the biosynthesis of bacterial sphingolipids and their role in host-commensal interactions (26, 36, 38, 42). Mutant strains of *Bacteroides fragilis* and *B. thetaiotaomicron* unable to produce sphingolipids show lower *in vitro* stress resistance, poor colonization phenotypes, and a failure to elicit anti-inflammatory host immune responses (35, 37, 38, 40, 43).

Although these *Bacteroides*-derived lipids play a key role in host inflammatory processes, their impact on OMV biogenesis and cargo selection remains unknown. We hypothesize that specific lipids selectively partition to OMVs, where they participate in the formation and recruitment of specific protein cargo, which could impact *Bacteroides*-host interactions. To test this hypothesis, we first performed a lipidomics analysis of the total membranes (TM) and OMVs from *B. thetaiotaomicron* VPI-5482. Our data show that OMVs contain diverse sphingolipids, glycerophospholipids, and glycine-serine dipeptide lipids (GS). The most abundant sphingolipids are ethanolamine phosphoceramide (EPC) and inositol phosphoceramide (IPC). Genetic approaches and mass spectrometry analysis allow the identification of the IPC biosynthetic pathway. Our results indicate that IPC sphingolipids do not exert significant effects on OMV biogenesis and, indeed, OMVs might serve as IPC delivery vehicles, contributing to the regulation of host-symbiont interactions.

RESULTS

OMVs contain sphingolipids, glycerophospholipids, and serine dipeptide lipids. In Bacteroidetes, the protein compositions of OMVs and the membranes from which they derive are strikingly different, with several proteins excluded from or exclusively present in OMVs (20–22, 44). We hypothesized that interaction of these proteins with lipids could be involved in the exclusion or recruitment of proteins into OMVs. In this model, it is conceivable that particular lipid species also partition between total membranes (TM) and OMVs. We employed a combination of liquid chromatography and untargeted mass spectrometry (LC-MS) to analyze the lipid contents from TM and OMVs produced by *B. thetaiotaomicron* VPI-5482. Mass-to-charge ratios (*m*/*z*) in

negative ion mode were utilized to assign each MS peak to the most probable lipid species. When required, we employed online resources from the publicly available LIPID MAPS Lipidomics Gateway (45–47) for prediction of the lipid species based on the *m/z* values. We determined that *B. thetaiotaomicron* OMVs contain sphingolipids, glycerophospholipids, and serine dipeptide lipids (Table S1). Our analyses showed minor differences in the lipid composition of TM and OMV fractions (Fig. 1). However, it revealed interesting features of OMV lipids.

The most ubiquitous lipid class found in bacteria, glycerophospholipids, is widely represented in TM and OMV fractions from *B. thetaiotaomicron* by the lipid species phosphatidylethanolamine (PE) (*m/z* values, 620.44, 634.5, 648.5, 662.5, 676.5) and phosphatidylinositol (PI) (*m/z* values, 767.5, 781.5, 795.5) (Fig. 1A). A remarkable feature of lipids from Bacteroidetes is the presence of acylated amino acids (48). Acylated amino acids such as ornithine lipid and commendamide have been found in other bacterial taxonomic groups (49, 50). Acylated glycine-serine dipeptide lipids (GS) have been found and studied in the Bacteroidetes taxons *Flavobacterium* spp., *Porphyromonas gingivalis*, and *B. thetaiotaomicron* (51–55). Our data showed that GS (*m/z* values, 639.5, 653.5) were present in both *B. thetaiotaomicron* TM and OMV fractions (Fig. 1B).

The most abundant lipid species found in OMVs were sphingolipids, mainly ceramide (*m/z* values, 600.4, 614.5, 628.5) and ceramide-derived compounds, including ethanolamine phosphoceramide (EPC) (*m/z* values, 663.5, 677.5, 691.5, 705.6) and inositol phosphoceramide (IPC) (*m/z* values, 796.5, 810.5, 824.6) (Fig. 1A; Table S1). EPC has been found in *B. fragilis*, *B. thetaiotaomicron*, and *Bacteroides ovatus* (56). IPC, a sphingolipid typically found in eukaryotes, has been discovered in *B. thetaiotaomicron* and *B. ovatus* (35, 38, 43). However, neither of the biosynthetic pathways of these sphingolipids has been elucidated.

Genetic basis of IPC synthesis. We postulated that sphingolipids may be involved in OMV biogenesis and sought to study OMVs in a mutant strain unable to produce this class of lipids. The first step in sphingolipid biosynthesis is the synthesis of 3-dehydroxysphinganine using palmitoyl-coenzyme A (CoA) and serine as the substrates via serine palmitoyl transferase (SPT). SPT orthologs are conserved in Bacteroidetes and carry the same function as in eukaryotes (35, 37, 39, 40, 43). Recent work has identified the *spt* ortholog in *B. thetaiotaomicron*, *BT0870*, and shown its essential function in sphingolipid biosynthesis (35). We generated a deletion strain for *spt* in *B. thetaiotaomicron* using a thymidine kinase (*tdk*) mutant strain as our wild-type (WT) genetic background, allowing for negative selection of transconjugants (57). Deletion of *spt*, as expected, resulted in a *B. thetaiotaomicron* strain unable to synthesize sphingolipids, as indicated by LC-MS (Fig. S1). The complete absence of sphingolipids caused a drastic reduction in bacterial growth and lysis, which made analysis of the contribution of OMV sphingolipids in *B. thetaiotaomicron* unfeasible (Fig. S1). Thus, we sought to investigate the roles of specific sphingolipids, such as EPC and IPC, in OMV formation. We performed BLAST analyses against the *B. thetaiotaomicron* VPI-5482 proteome using amino acid sequences from eukaryotic EPC and IPC synthases (CPES from *Drosophila melanogaster* and AUR1 from *Saccharomyces cerevisiae*). While no matches were found for EPC synthase, we found a putative ortholog in *B. thetaiotaomicron*, *BT1522*, predicted to encode an IPC synthase. Analysis of the genes surrounding *BT1522* suggested that *BT1522* is part of an operon composed of genes *BT1522* to *BT1526* (35). We employed PSI-BLAST, HHpred, and Phyre2 to interrogate the function of the predicted proteins encoded by the *BT1522–1526* operon (Fig. 2A) and generate a predicted IPC biosynthetic pathway (Fig. 2B) (58–60). *BT1526* is annotated as a myo-inositol-phosphate synthase, an enzyme that generates myo-inositol-3-phosphate from glucose-6-P (Fig. 2B) (61, 62). Myo-inositol 3-phosphate is the building block for most phosphoinositol-derived compounds (61, 62). *BT1525* is predicted to encode a phosphatidylglycerol-1-phosphate (PGP) phosphatase, an enzyme that generates phosphatidylglycerol using PGP as the substrate (Fig. 2A) (63). *BT1524* is predicted to encode a GtrA-like protein, an inner membrane protein that seems to be required for synthesis of lipid-linked

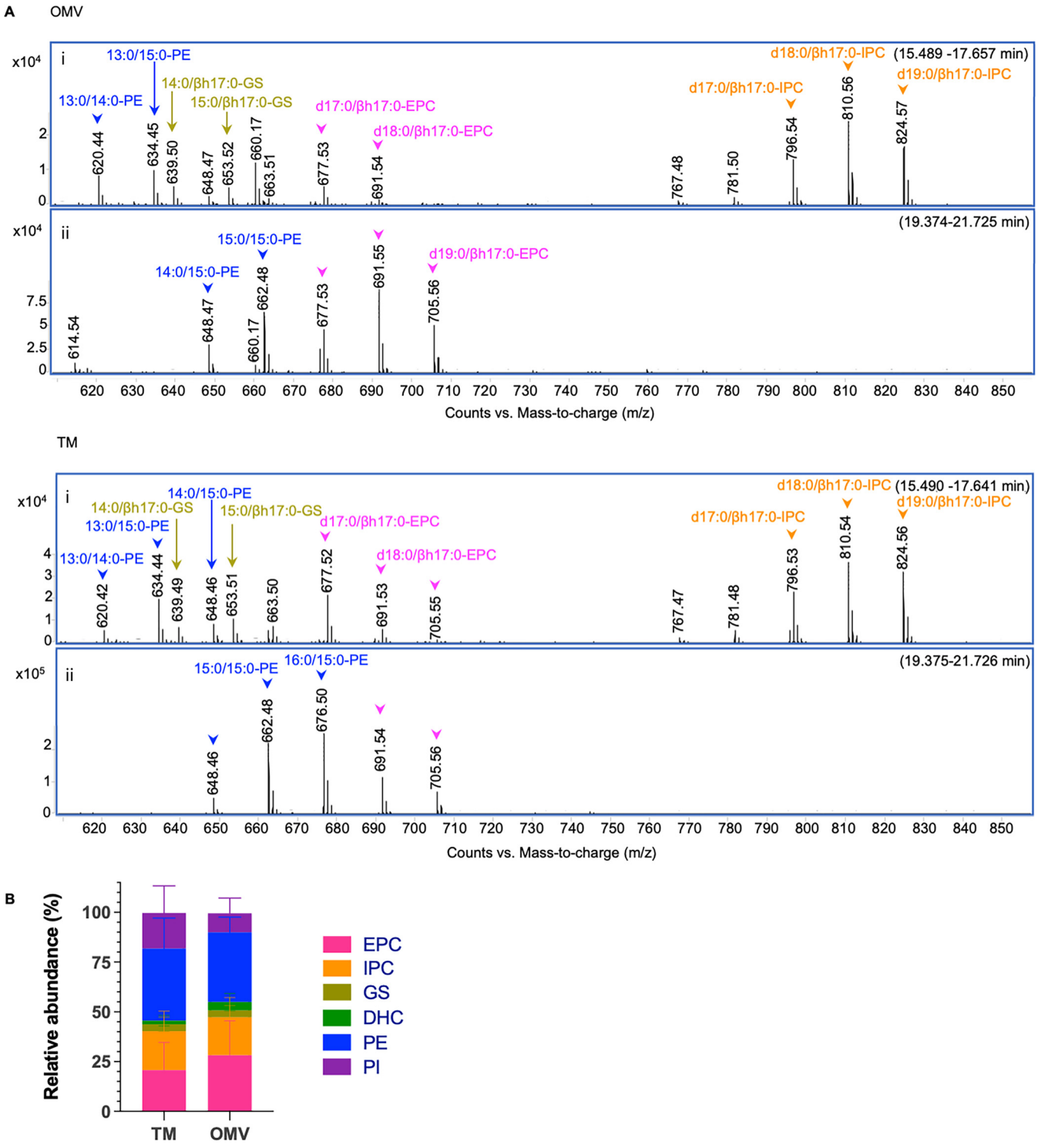

FIG 1 Lipid species diversity and distribution in OMVs and TM from *B. thetaiotaomicron*. Label-free quantification using LC-MS of lipid species from OMVs and TM of wild-type *B. thetaiotaomicron*. (A) ESI MS spectra showing absolute counts of the $[M–H]^-$ ions of various lipids (mainly sphingonoids) from extracts of OMV (upper panels) and TM (lower panels) and the signal averaged spectra of LC fractions 15.5 to 17.6 (i) and 19.4 to 21.7 (ii) min, respectively. IPC, inositol phosphoceramide; EPC, ethanolamine phosphoceramide; PE, phosphatidylethanolamine; PI, phosphatidylinositol; DHC, dihydroceramide; GS, glycine-serine dipeptide lipids. The fatty acyl chain, e.g., "15:0/βh17:0," indicates "C15 fatty acyl (FA) chain with no double bond" and "C17 chain with β-hydroxy side chain with no double bond," respectively. "d17:0" represents "dihydroxy-17:0 LCB" (LCB, long-chain base). (B) Relative abundance of the most represented lipid species as a percentage of the total lipid composition for each fraction. The assigned structures (as labeled in each section in panel A) are based on tandem MS analysis of the individual ions, and the designation of the structures is according to LIPID MAPS with modifications. The graph shows the median values and standard deviation of four biological replicates.

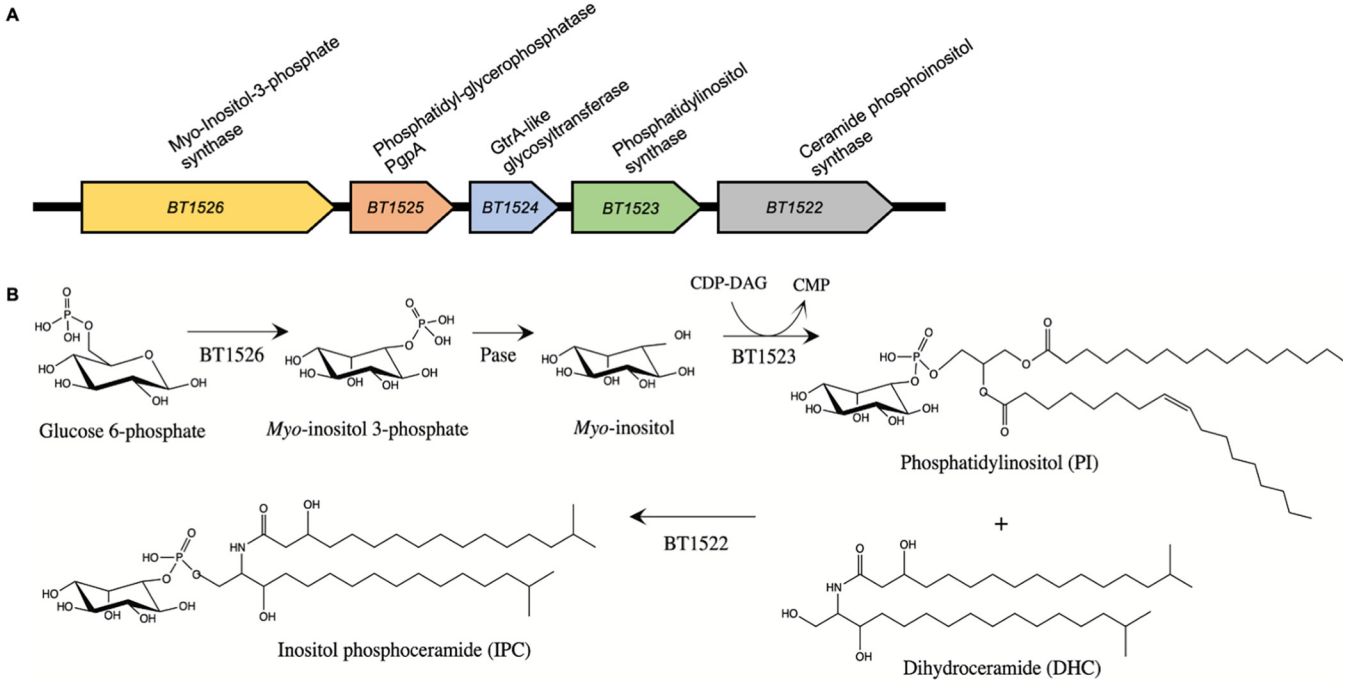

FIG 2 Proposed genes and pathway for IPC synthesis. (A) Schematic representation of the *BT1522–1526* hypothetical IPC biosynthesis operon with the predicted gene function estimated by PSI-BLAST, HHpred, and Phyre2 analysis. (B) Schematic overview of the predicted IPC biosynthetic pathway. Pase, phosphatase.

glycans in bacteria (64–66). *BT1523* is predicted to encode a phosphatidylinositol (PI) synthase, which utilizes inositol and cytidine diphosphate (CDP)-diacylglycerol to synthesize phosphatidylinositol (Fig. 2B) (67). Finally, an IPC synthase (*BT1522*) generates IPC in eukaryotes using ceramide and phosphatidylinositol as the substrates (Fig. 2B) (68, 69). To generate clean deletion mutant strains for genes *BT1522* to *BT1526*, we employed the thymidine kinase (*tdk*) mutant strain as our wild-type genetic background. We were able to obtain mutant strains for genes *BT1522*, *BT1523*, *BT1524*, and *BT1526*. Deletion mutants for the *BT1525* gene could not be obtained after many rounds of negative selection, suggesting that *BT1525* is an essential gene in *B. thetaiotaomicron*. Lipid analyses by LC-MS of TM and OMVs showed no IPC content in the *BT1523* mutant and negligible IPC levels ($<$1% relative abundance) for the *BT1522* and *BT1526* mutants (Fig. 3, Fig. S2; Table S1) in both the TM and OMV fractions (Fig. 4). The *BT1524* mutant strain showed significantly lower IPC relative abundance than the wild-type strain in both fractions (Fig. 4). Conversely, the *BT1524* mutant displayed higher relative abundance levels of PI in the TM than the wild-type strain (Fig. 4), suggesting that *BT1524* impacts the synthesis of IPC through an unknown mechanism. PI was not detected in the *BT1523* and *BT1526* mutants in either fraction, in agreement with their predicted functions in PI biosynthesis. The *BT1522* mutant strain displayed relative abundance levels of PI indistinguishable from those of the wild-type strain (Fig. 4). In agreement with abolished IPC synthesis, membranes from the *BT1522*, *BT1523*, and *BT1526* strains displayed higher levels of ceramides than wild-type and *BT1524* mutant strains (Table S1). The mutants in the IPC displayed mild growth defects (Fig. S3). Complementation of the *BT1522–1526* mutated genes restored the IPC lipid profiling in all the individual mutants (Fig. 3, right panel), confirming that the operon is necessary and sufficient for IPC biosynthesis in *B. thetaiotaomicron*.

Depletion of IPC does not affect OMV biogenesis or cargo. IPC could be required for OMV biogenesis, or alternatively it could mediate interactions with proteins, impacting the OMV cargo. We analyzed *B. thetaiotaomicron* cells and OMV preparations using transmission electron microscopy (TEM) and found no obvious differences in morphology between wild-type and IPC mutant strains (Fig. 5A; Fig. S4). We also

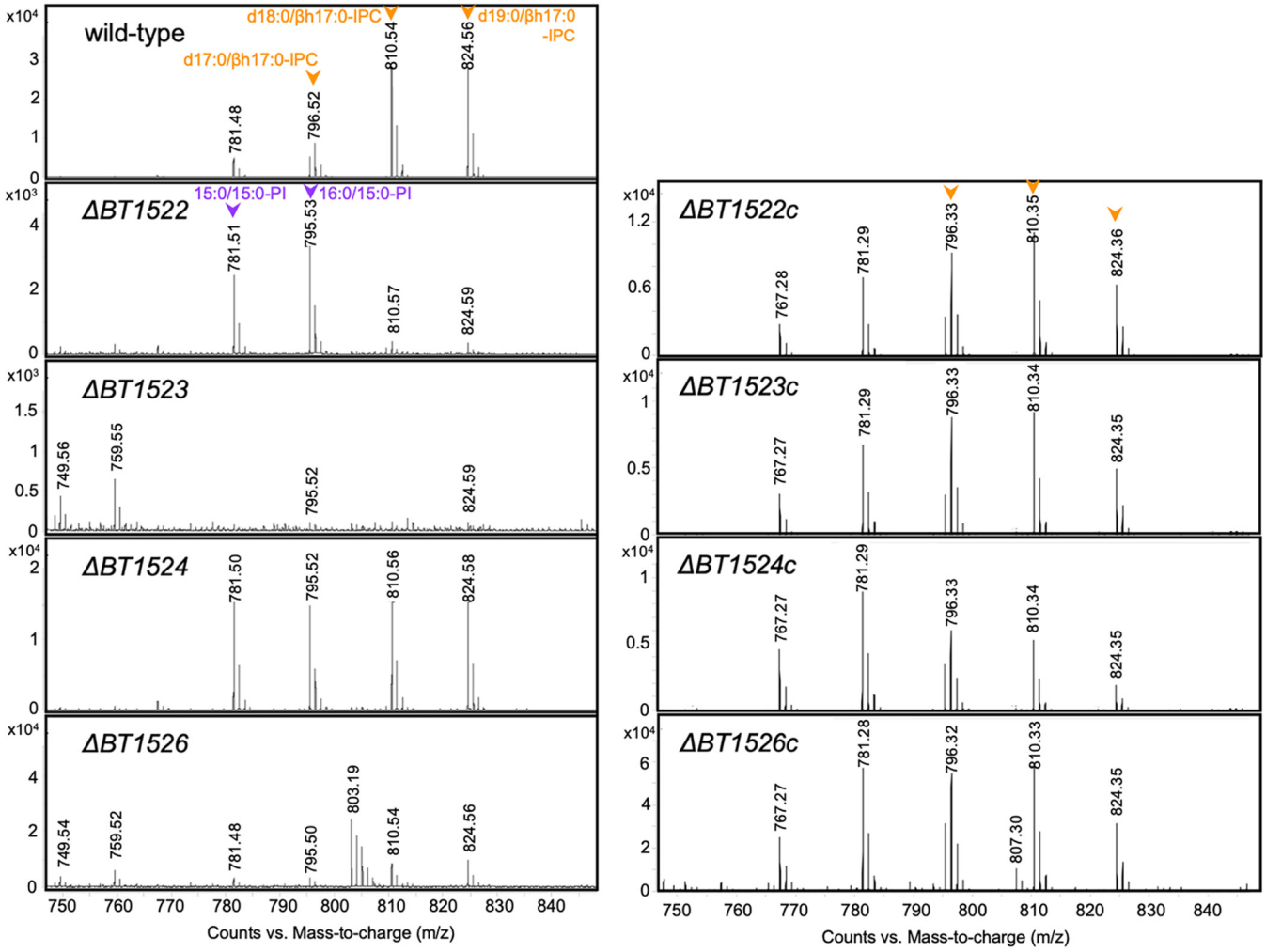

FIG 3 ESI MS spectra showing absolute counts of the $[M–H]^-$ ions of IPC and PI molecules of TM lipids extracted from wild-type and *BT1522–1526* mutants (left panel) and their complemented strains (right panel). The orange arrows indicate IPC lipid species; the purple arrows indicate PI lipid species. The graphs are representative of three biological replicates.

found similar levels of vesiculation, vesicles sizes, and OMV protein concentration among all strains (Fig. S4 and Fig. 5B). Analysis of TM and OMV protein contents using SDS-PAGE and Coomassie blue stain showed indistinguishable protein band patterns between the wild-type and *BT1522–1526* mutant strains (Fig. 6A). Western blot assays of the TM and OMV fractions revealed that, despite their mild growth defects, the mutant strains do not lyse spontaneously, as evidenced by the lack of RNA polymerase signal in OMV preparations (Fig. 6B).

As mentioned, *Bacteroides* preferentially packs OMVs with certain lipoproteins that are mainly acidic and have hydrolytic activity, resulting in the selection of cargo components and the exclusion of other abundant OM proteins (21, 22, 44). To examine whether *BT1522–1526* mutant strains have an impact on protein cargo selection, we analyzed SusG secretion into OMVs in the different strains. SusG is a lipoprotein with amylase activity that has previously been shown to be preferentially packaged into OMVs (22). Western blot assays of TM and OMV fractions of the different mutants revealed no differences in SusG packaging into OMVs (Fig. S5). Together, these data rule out a major role for IPC in OMV formation or cargo selection.

DISCUSSION

In this work, we determined the lipid composition of OMVs produced by *B. thetaiotaomicron*. LC-MS analysis demonstrated that sphingolipid species represent more than

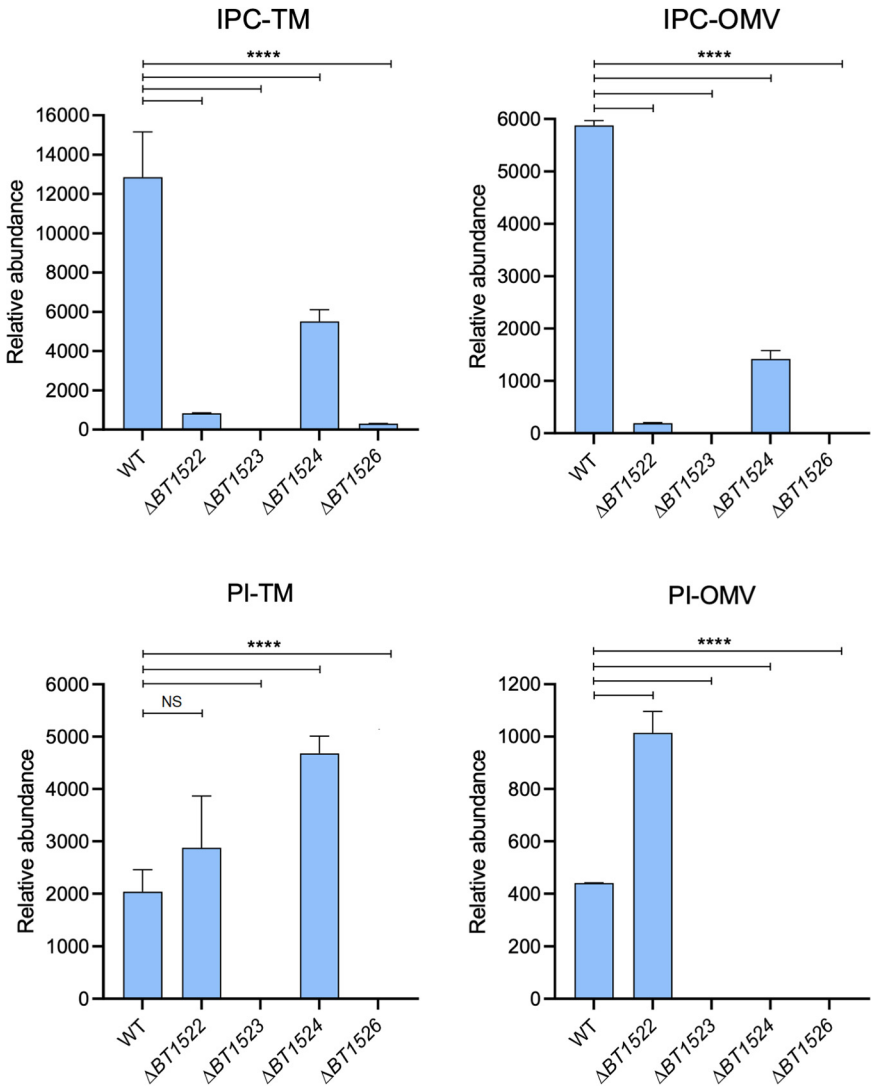

FIG 4 Relative abundances of IPC and PI species from TM and OMV fractions. The graphs show the median values of two biological replicates with the range for individual lipid species from each sample. Analysis of variance (ANOVA) tests were used to determine the statistical significance with an alpha value of 0.05; ****, $P < 0.0001$.

50% of the total lipid content of OMVs. Among these, EPC and IPC were the most abundant sphingolipids. We determined that the *BT1522-1526* operon is essential for the synthesis of PI and IPC, the latter being the second most abundant sphingolipid species in OMV fractions. *BT1522–1526* mutant strains lacking IPC displayed mild growth defects, but their OMV secretion phenotypes were indistinguishable from that of the wild-type strain. Furthermore, protein cargo selection into OMVs was not affected in the different mutants analyzed, indicating that IPC is not required for OMV biogenesis.

The results from this study indicate that the protein encoded by *BT1522* is the main IPC synthase in *B. thetaiotaomicron*. Remarkably, the detection of very low levels of IPC in membranes from the *BT1522* mutant strain suggests partial redundancy by an unknown enzyme that could be acting as an IPC synthase in a suboptimal manner. Moreover, higher levels of dihydroceramide and dehydrated ceramide (Table S1) in the *BT1522*, *BT1523*, and *BT1526* mutants in comparison to those in the wild-type and *BT1524* strains strongly suggest that these lipid molecules are the precursors for IPC synthesis in *B. thetaiotaomicron*. Intriguingly, our results have also shown that in the

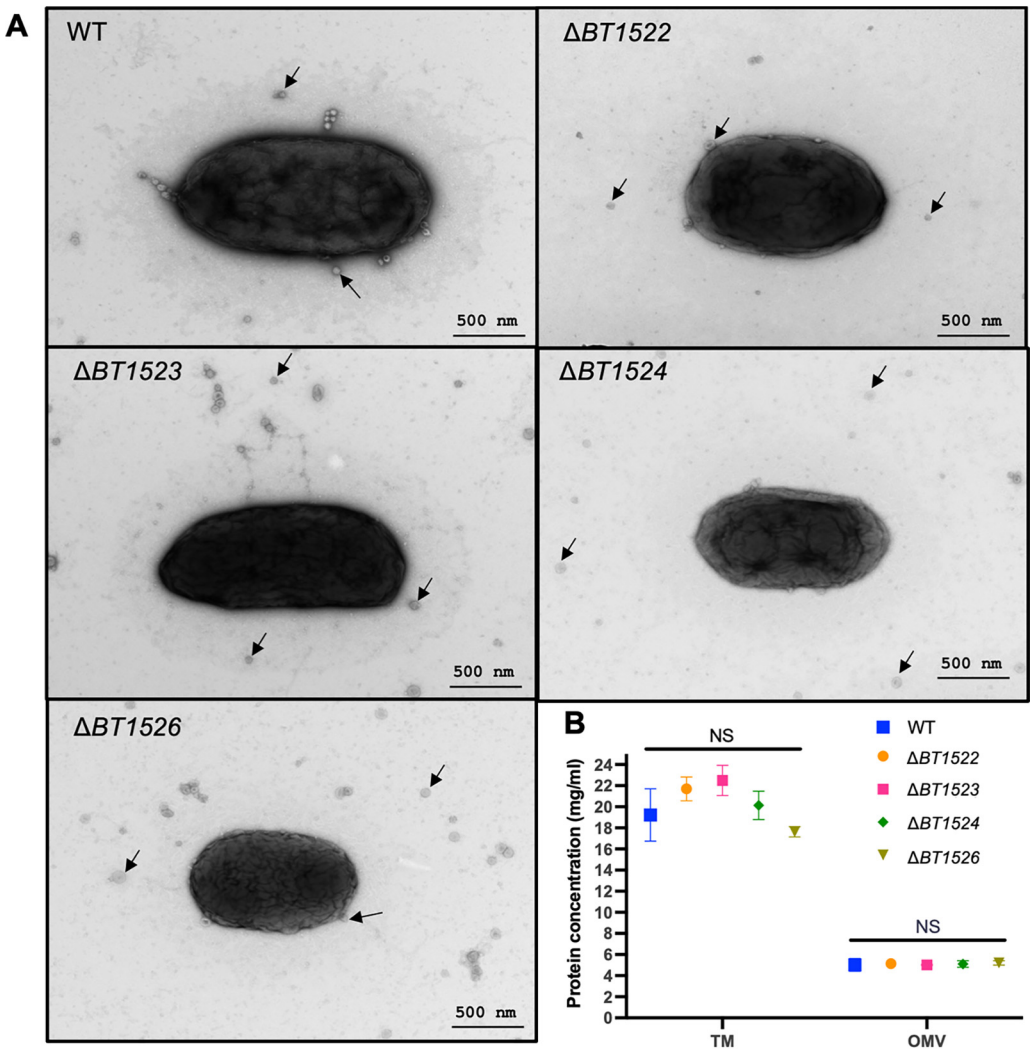

FIG 5 (A) Transmission electron microscopy of *B. thetaiotaomicron* wild-type (WT) and Δ*BT1522–1526* strains showing no significant differences in shape. The strains were grown on BHI agar plates, and bacterial lawns were swabbed from the surface of the plates and resuspended in PBS for imaging by TEM. These images were acquired from Wandy Beatty at the WUSTL Molecular Microbiology Imaging Facility. Magnification of 20,000× is shown. (B) TM and OMV fractions were prepared using early stationary-phase liquid-grown cultures of WT and Δ*BT1522–1526* strains. The TM and OMV preparations were resuspended in PBS for each strain, and the total protein concentration was determined. The graph shows the means and error bars by standard deviation (SD) of 3 biological replicates for each strain. Statistical significance was determined by *t* test (*P* value, <0.05).

BT1524 mutant, the PI accumulation in TM was not reflected in the OMV fraction, as was observed in the *BT1522* mutant (Fig. 4, lower panels). Future work will help to elucidate the function of *BT1524* in IPC synthesis and whether it is linked to the selection of OMV lipid cargo in *B. thetaiotaomicron*.

Regarding the impact of PI/IPC on cell growth, our results suggest that while a lack of IPC partially impacts the exponential growth phase, its absence could have a role in survival after reaching the stationary phase. *P. gingivalis*, *B. fragilis*, and *B. thetaiotaomicron* lacking SPT activity display a reduction in growth and post-stationary-phase viability, suggesting that IPC could be mediating this phenotype in *B. thetaiotaomicron* (37, 39).

Regarding other lipids with potential signaling activities within the host milieu, our results showed very similar levels of GS between TM and OMVs. A recent study has shown that the gene *glsB* (*BT3459*) from *B. thetaiotaomicron* is required for the synthesis of GS, providing a partial genetic basis for amino lipid production in Bacteroidetes (55).

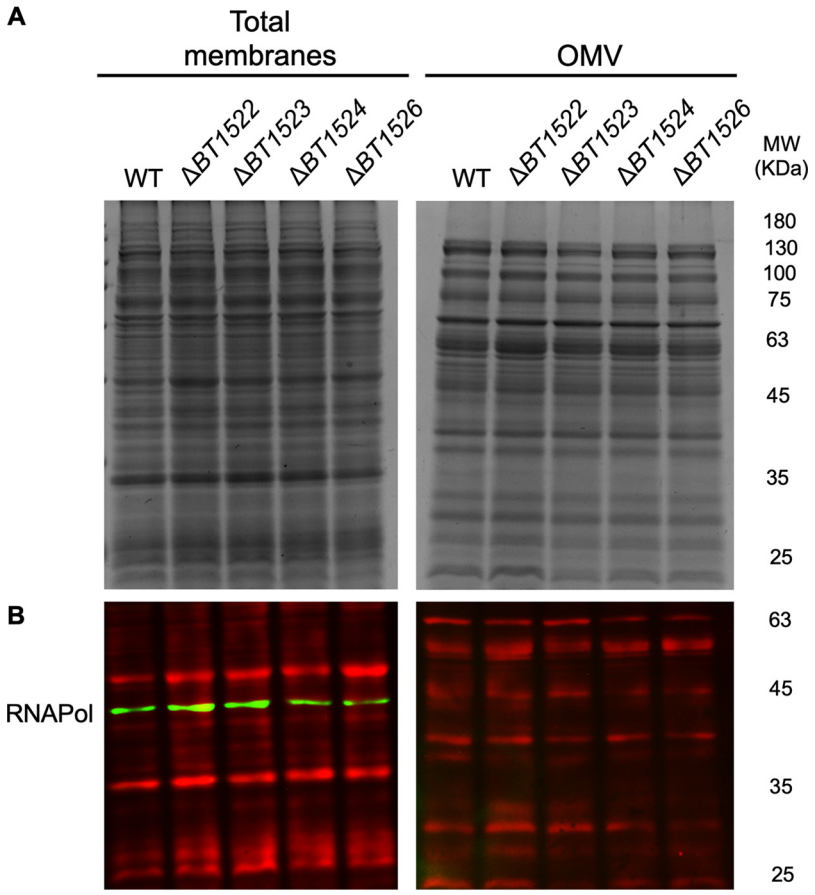

FIG 6 TM and OMV fractions were prepared using early stationary-phase liquid-grown cultures. The TM and OMV preparations were resuspended in PBS, and the protein concentration was determined: 10 μg protein per sample was loaded onto 12% SDS-PAGE gels and analyzed by (A) Coomassie blue staining or (B) Western blot, using anti-RNA polymerase antisera and REVERT total protein stain as the loading control. Lack of IPC does not cause cell lysis or impact the differential TM/OMV protein profile.

Similar to sphingolipids, GS are also required for bacterial homeostasis and colonization of the murine gut (55). A specific serine-containing lipid from *P. gingivalis*, called lipid 654, can be cleaved by host phospholipases into lipid 430, a highly inflammatory derivative (52). Amino lipids signal inflammation through host TLR2 receptors and have been proposed as markers of atherosclerosis (52, 53, 70, 71). Nevertheless, the potential contributions of amino lipids to OMV formation and gut inflammation by *B. thetaiotaomicron* are still unknown. The majority of *B. thetaiotaomicron* cells reside within the colonic mucus layer in mice, and a small proportion localize within colonic crypts in close association to epithelial cells (72–76). Data from irritable bowel disease (IBD) patients show that a decrease in *Bacteroides* sphingolipids is negatively correlated with an increase in host ceramides, in comparison to a healthy human cohort (13, 35). Recent data from the Ley group has showed that sphingolipids from *Bacteroides* are likely to be incorporated *in vivo* into colonic epithelial cells and modify the host glucose metabolism (77). *In vitro* studies in *P. gingivalis* also showed the incorporation of bacterial sphingolipids into THP I human cell lines in a contact-independent manner and a decreased inflammatory response from the host cell compared to that in SPT-deficient strains (40, 78). Altogether, these results indicate that sphingolipid-enriched OMVs act as carriers of secreted anti-inflammatory signals within the colonic niche and are taken up by host colonocytes (79). This mechanism of sphingolipid delivery could bypass the distance imposed by the colonic mucus barrier between *Bacteroides* cells and colonic epithelial cells. Our data, along

with the work of others, show an opportunity to use targeted sphingolipid-deficient bacterial strains to genetically dissect the contribution of the *Bacteroides* sp. cell envelope to colonic homeostasis and gut symbiosis. *B. fragilis*, the *Bacteroides* species most frequently isolated from anaerobic infections in humans, lacks a *BT1522–1526* orthologous region in its genome. Gain-of-function experiments incorporating genes from the *BT1522–1526* region into a different *Bacteroides* species such as *B. fragilis* could contribute to dissecting the role of IPC synthesis genes in a heterologous context. While sphingolipids are the main lipid components of *Bacteroides* sp. membranes, we and others have shown that lipid repertoires vary according to the species analyzed (35, 37, 38, 43, 77). We thus hypothesize that any contributions of *Bacteroides* sphingolipids to health or disease states will likely be governed by the species composition and relative abundance within each host microbiome.

MATERIALS AND METHODS

Bacterial strains and growth conditions. Oligonucleotides, strains, and plasmids are described in Table S2 in the supplemental material. *Escherichia coli* strains were grown in lysogenic broth (LB) or on LB agar plates. *Bacteroides* strains were grown in an anaerobic chamber (Coy Laboratories) using an atmosphere of 10% H_2, 5% CO_2, 85% N_2. For liquid and solid growth, brain heart infusion (BHI) or BHI agar plates supplemented with hemin and vitamin K3 were used. Antibiotics and other compounds were used as follows: ampicillin at 100 μg/mL, erythromycin at 25 μg/mL, and bromodeoxyuridine at 200 μg/mL. For growth curves, overnight cultures of *B. thetaiotaomicron* wild-type and mutant strains were back-diluted into 96-well plates using BHI equilibrated to an anaerobic atmosphere. A final volume of 0.2 mL per well was used, and the optical density at 600 nm (OD_{600}) was adjusted to 0.1. Plates containing an anaerobic atmosphere were sealed with non-gas permeable transparent film and incubated at 37°C inside a temperature-controlled plate reader (Synergy HTX, BioTek Instruments). OD_{600} measurements were taken every 15 min.

Construction of plasmids, mutagenesis, generation of mutants by clean deletion and complementation. Generation of *B. thetaiotaomicron* deletion strains was carried out using the Δ*tdk* strategy as previously described (57). Briefly, 1,000-bp upstream and downstream fragments of *BT0870*, *BT1522*, *BT1523*, *BT1524*, *BT1525*, and *BT1526* were cloned into the pExchange-*tdk* vector using *E. coli* S17-1 λpir as the cloning strain. Constructs were conjugated into *B. thetaiotaomicron* Δ*tdk* cells using previously transformed *E. coli* S17-1 λpir as the donor, and strain plating and selection were performed as previously described (57).

For complementation of the mutant strains, *BT1522*, *BT1523*, *BT1524*, and *BT1526* were PCR amplified and purified. Each fragment was cloned into the pWW3867 integrative plasmid backbone using the Gibson DNA assembly method (NEB) (72). *E. coli* S17-1 λpir was used as the cloning strain, and each construct was conjugated into the corresponding *B. thetaiotaomicron* Δ*BT1522–1526* mutant strains (Table S2). Positive transformants were selected by antibiotic resistance as described previously (57).

OMV preparations. Crude OMVs were obtained by ultracentrifugation of the filtered spent medium from 150 mL of liquid culture as described (21). Briefly, 18- to 20-h cultures of *B. thetaiotaomicron* were centrifuged at 6,500 rpm at 4°C for 10 min. To remove residual cells, the supernatant was filtered using a 0.22-mm-pore membrane (Millipore). The filtrate was subjected to ultracentrifugation at 200,000 × *g* for 2 h (Optima L-100 XP ultracentrifuge; Beckman Coulter). The supernatant was discarded, and the pellets containing the OMV preparation were resuspended in phosphate-buffered saline (PBS) and normalized by OD before protein and lipid analyses. The OMV amount was estimated by measuring the protein content using a DC protein assay kit (Bio-Rad). Fractions were aliquoted and stored at −80°C until analyzed.

Membrane preparations. Total membrane preparations were obtained by cell lysis and ultracentrifugation as previously described (21). The total membranes from 150 mL of liquid culture were resuspended in PBS using a 2-mL glass tissue grinder with a polytetrafluoroethylene (PTFE) pestle (VWR). The protein content was quantified using a DC protein assay kit (Bio-Rad). The fractions were aliquoted and stored at −80°C until analysis.

Total lipid extractions. Total lipids from OMVs and TM were extracted based on the Bligh and Dyer chloroform:methanol method (80). Briefly, 2 volumes of methanol, 1 volume of chloroform, and 0.8 volumes of Milli-Q water were added to 1 volume of PBS-resuspended OMV or TM fractions in solvent-resistant glass tubes. The contents were mixed for 1 min by vortexing, and 1 volume of chloroform was added to the mixture. The contents were mixed for another minute, and the tubes were centrifuged for 5 min at 4,000 rpm. After centrifugation, the bottom phase (organic) was recovered using a glass Pasteur pipette and stored in solvent-sealed vials at −80°C until lipid analysis by LC-MS.

LC-MS analysis of lipids from TM and OMVs. Untargeted LC/MS analyses were conducted on an Agilent 6550 A QTOF instrument with an Agilent 1290 high-performance liquid chromatograph (HPLC) with an autosampler, operated using Agilent MassHunter software (Santa Clara, CA, USA). Separation of the total lipid extracts was achieved using a Thermo Fisher (Waltham, MA, USA) BETASIL C_{18} column (100 × 2.1 mm, 5 μm) at a flow rate of 300 μL/min at room temperature. The mobile phase contained 5 mM ammonium formate (pH 5.0) both in solvent A, acetonitrile:water (60:40, vol/vol), and solvent B, isopropanol:acetonitrile (90:10, vol/vol). A gradient elution was applied in the following manner: 68% A, 0 to 1.5 min; 68 to 55% A, 1.5 to 4 min; 55 to 48% A, 4 to 5 min; 48 to 42% A, 5 to 8 min; 42 to 34% A, 8 to 11 min; 34 to 30% A, 11 to 14 min; 30 to 25% A, 14 to 18 min; 25 to 3% A, 18 to 23 min; 3 to 0% A, 25 to 30 min; 0% A, 30 to 35 min; 68% A, 35 to 40 min. Both the positive-ion and negative-ion electrospray ionization (ESI) MS scans were acquired in the mass range

of 200 to 2,000 Da at a rate of 2 scans/min. High-resolution (R = 100,000 at m/z 400) mass spectrometric analyses of the lipid extracts were also conducted on a Thermo LTQ Orbitrap Velos. Lipids were loop injected into the ESI ion source using a built-in syringe pump which was set to continuously deliver a flow of 20 μL/min methanol with 0.5% NH_4OH. The scanned mass spectra were recalibrated internally with a known mass, namely, 13:0/15:0 PE at m/z 634.4453. Linear ion trap (LIT) multistage MS (MS^n) spectra were obtained for structural identification as described previously (81–83).

Transmission electron microscopy. For negative staining and analysis by TEM, bacterial suspensions in PBS or OMV were allowed to absorb onto freshly glow-discharged Formvar/carbon-coated copper grids for 10 min. The grids were washed in distilled water and stained with 1% aqueous uranyl acetate (Ted Pella, Inc., Redding, CA) for 1 min. Excess liquid was gently wicked off, and the grids were allowed to air dry. The samples were viewed on a 1200EX transmission electron microscope (JEOL USA, Peabody, MA) equipped with an 8-megapixel digital camera (Advanced Microscopy Techniques, Woburn, MA).

SDS-PAGE and Western blot analysis. The total membrane and OMV fractions were analyzed using standard 12% Tris-glycine SDS-PAGE gels. Briefly, 10 μg of TM or OMV fractions were loaded onto SDS-PAGE gels in duplicate. One gel was stained with Coomassie blue to visualize the protein band patterns. The other gel was transferred onto a 0.45-μm nitrocellulose membrane (Bio-Rad), and Western blotting was performed using the LI-COR system. After transfer of the protein preparations from the SDS-PAGE gels, nitrocellulose membranes were incubated with REVERT total protein stain as described by the manufacturer (LI-COR) and imaged immediately at 680 nm. The membranes were blocked using Tris-buffered saline (TBS)-based 3% nonfat milk blocking solution. The primary antibodies used in this study were mouse monoclonal anti-*E. coli* RNA polymerase (RNApol) subunit alpha (BioLegend). The secondary antibodies used were IRDye antimouse 780 antibodies (LI-COR). Imaging was performed using an Odyssey CLx scanner (LI-COR).

Data availability. The resulting lipidomic data are available at the NIH Common Fund's National Metabolomics Data Repository (NMDR) website, https://www.metabolomicsworkbench.org (84), where they have been assigned project ID PR001199. The data can be accessed directly via https://doi.org/10.21228/M8QQ5J.

SUPPLEMENTAL MATERIAL

Supplemental material is available online only.

SUPPLEMENTAL FILE 1, PDF file, 3 MB.

SUPPLEMENTAL FILE 2, XLSX file, 0.1 MB.

ACKNOWLEDGMENTS

We thank all members of the Feldman lab for valuable discussions. We also thank Clay Jackson-Litteken and Jenna McGuffey for critically reading the manuscript. Furthermore, we thank Wandy Beatty for assistance with the TEM experiments.

This work was supported by NIH grant R21AI151873.

M.F.F., E.V., and M.G.S. designed and wrote the manuscript. E.V. and M.G.S. performed experiments on *B. thetaiotaomicron*. F.-F.H. performed the MS lipid experiments and data analysis.

REFERENCES

1. Human Microbiome Project Consortium. 2012. Structure, function and diversity of the healthy human microbiome. Nature 486:207–214. https://doi.org/10.1038/nature11234.
2. Yatsunenko T, Rey FE, Manary MJ, Trehan I, Dominguez-Bello MG, Contreras M, Magris M, Hidalgo G, Baldassano RN, Anokhin AP, Heath AC, Warner B, Reeder J, Kuczynski J, Caporaso JG, Lozupone CA, Lauber C, Clemente JC, Knights D, Knight R, Gordon JI. 2012. Human gut microbiome viewed across age and geography. Nature 486:222–227. https://doi.org/10.1038/nature11053.
3. Mombaerts P, Mizoguchi E, Grusby MJ, Glimcher LH, Bhan AK, Tonegawa S. 1993. Spontaneous development of inflammatory bowel disease in T cell receptor mutant mice. Cell 75:275–282. https://doi.org/10.1016/0092-8674(93)80069-Q.
4. Mazmanian SK, Liu CH, Tzianabos AO, Kasper DL. 2005. An immunomodulatory molecule of symbiotic bacteria directs maturation of the host immune system. Cell 122:107–118. https://doi.org/10.1016/j.cell.2005.05.007.
5. Lathrop SK, Bloom SM, Rao SM, Nutsch K, Lio C-W, Santacruz N, Peterson DA, Stappenbeck TS, Hsieh C-S. 2011. Peripheral education of the immune system by colonic commensal microbiota. Nature 478:250–254. https://doi.org/10.1038/nature10434.
6. Gensollen T, Iyer SS, Kasper DL, Blumberg RS. 2016. How colonization by microbiota in early life shapes the immune system. Science 352:539–544. https://doi.org/10.1126/science.aad9378.
7. Zhao Q, Elson CO. 2018. Adaptive immune education by gut microbiota antigens. Immunology 154:28–37. https://doi.org/10.1111/imm.12896.
8. Ridaura VK, Faith JJ, Rey FE, Cheng J, Duncan AE, Kau AL, Griffin NW, Lombard V, Henrissat B, Bain JR, Muehlbauer MJ, Ilkayeva O, Semenkovich CF, Funai K, Hayashi DK, Lyle BJ, Martini MC, Ursell LK, Clemente JC, Van Treuren W, Walters WA, Knight R, Newgard CB, Heath AC, Gordon JI. 2013. Gut microbiota from twins discordant for obesity modulate metabolism in mice. Science 341:1241214. https://doi.org/10.1126/science.1241214.
9. Arrieta M-C, Stiemsma LT, Amenyogbe N, Brown EM, Finlay B. 2014. The intestinal microbiome in early life: health and disease. Front Immunol 5:427. https://doi.org/10.3389/fimmu.2014.00427.
10. Arrieta M-C, Stiemsma LT, Dimitriu PA, Thorson L, Russell S, Yurist-Doutsch S, Kuzeljevic B, Gold MJ, Britton HM, Lefebvre DL, Subbarao P, Mandhane P, Becker A, McNagny KM, Sears MR, Kollmann T, Mohn WW, Turvey SE, Finlay BB, CHILD Study Investigators. 2015. Early infancy microbial and metabolic alterations affect risk of childhood asthma. Sci Transl Med 7:307ra152. https://doi.org/10.1126/scitranslmed.aab2271.
11. Tamburini S, Shen N, Wu HC, Clemente JC. 2016. The microbiome in early life: implications for health outcomes. Nat Med 22:713–722. https://doi.org/10.1038/nm.4142.
12. Franzosa EA, Sirota-Madi A, Avila-Pacheco J, Fornelos N, Haiser HJ, Reinker S, Vatanen T, Hall AB, Mallick H, McIver LJ, Sauk JS, Wilson RG, Stevens BW, Scott JM, Pierce K, Deik AA, Bullock K, Imhann F, Porter JA, Zhernakova A, Fu J, Weersma RK, Wijmenga C, Clish CB, Vlamakis H, Huttenhower C, Xavier RJ. 2019. Gut microbiome structure and metabolic activity in inflammatory bowel disease. Nat Microbiol 4:293–305. https://doi.org/10.1038/s41564-018-0306-4.

13. Schirmer M, Garner A, Vlamakis H, Xavier RJ. 2019. Microbial genes and pathways in inflammatory bowel disease. Nat Rev Microbiol 17:497–511. https://doi.org/10.1038/s41579-019-0213-6.
14. Foley MH, Cockburn DW, Koropatkin NM. 2016. The Sus operon: a model system for starch uptake by the human gut Bacteroidetes. Cell Mol Life Sci 73:2603–2617. https://doi.org/10.1007/s00018-016-2242-x.
15. Delday M, Mulder I, Logan ET, Grant G. 2019. Bacteroides thetaiotaomicron ameliorates colon inflammation in preclinical models of Crohn's disease. Inflamm Bowel Dis 25:85–96. https://doi.org/10.1093/ibd/izy281.
16. Bloom SM, Bijanki VN, Nava GM, Sun L, Malvin NP, Donermeyer DL, Dunne WM, Allen PM, Stappenbeck TS. 2011. Commensal Bacteroides species induce colitis in host-genotype-specific fashion in a mouse model of inflammatory bowel disease. Cell Host Microbe 9:390–403. https://doi.org/10.1016/j.chom.2011.04.009.
17. Hickey CA, Kuhn KA, Donermeyer DL, Porter NT, Jin C, Cameron EA, Jung H, Kaiko GE, Wegorzewska M, Malvin NP, Glowacki RWP, Hansson GC, Allen PM, Martens EC, Stappenbeck TS. 2015. Colitogenic Bacteroides thetaiotaomicron antigens access host immune cells in a sulfatase-dependent manner via outer membrane vesicles. Cell Host Microbe 17:672–680. https://doi.org/10.1016/j.chom.2015.04.002.
18. Wegorzewska MM, Glowacki RWP, Hsieh SA, Donermeyer DL, Hickey CA, Horvath SC, Martens EC, Stappenbeck TS, Allen PM. 2019. Diet modulates colonic T cell responses by regulating the expression of a Bacteroides thetaiotaomicron antigen. Sci Immunol 4:eaau9079. https://doi.org/10.1126/sciimmunol.aau9079.
19. Hsieh S, Porter NT, Donermeyer DL, Horvath S, Strout G, Saunders BT, Zhang N, Zinselmeyer B, Martens EC, Stappenbeck TS, Allen PM. 2020. Polysaccharide capsules equip the human symbiont Bacteroides thetaiotaomicron to modulate immune responses to a dominant antigen in the intestine. J Immunol 204:1035–1046. https://doi.org/10.4049/jimmunol.1901206.
20. Rakoff-Nahoum S, Coyne MJ, Comstock LE. 2014. An ecological network of polysaccharide utilization among human intestinal symbionts. Curr Biol 24:40–49. https://doi.org/10.1016/j.cub.2013.10.077.
21. Elhenawy W, Debelyy MO, Feldman MF. 2014. Preferential packing of acidic glycosidases and proteases into Bacteroides outer membrane vesicles. mBio 5:e00909-14. https://doi.org/10.1128/mBio.00909-14.
22. Valguarnera E, Scott NE, Azimzadeh P, Feldman MF. 2018. Surface exposure and packing of lipoproteins into outer membrane vesicles are coupled processes in Bacteroides. mSphere 3:e00559-18. https://doi.org/10.1128/mSphere.00559-18.
23. Toyofuku M, Nomura N, Eberl L. 2019. Types and origins of bacterial membrane vesicles. Nat Rev Microbiol 17:13–24. https://doi.org/10.1038/s41579-018-0112-2.
24. Shen Y, Giardino Torchia ML, Lawson GW, Karp CL, Ashwell JD, Mazmanian SK. 2012. Outer membrane vesicles of a human commensal mediate immune regulation and disease protection. Cell Host Microbe 12:509–520. https://doi.org/10.1016/j.chom.2012.08.004.
25. Hampton CM, Guerrero-Ferreira RC, Storms RE, Taylor JV, Yi H, Gulig PA, Wright ER. 2017. The opportunistic pathogen *Vibrio vulnificus* produces outer membrane vesicles in a spatially distinct manner related to capsular polysaccharide. Front Microbiol 8:2177. https://doi.org/10.3389/fmicb.2017.02177.
26. Heaver SL, Johnson EL, Ley RE. 2018. Sphingolipids in host–microbial interactions. Curr Opin Microbiol 43:92–99. https://doi.org/10.1016/j.mib.2017.12.011.
27. Stankeviciute G, Guan Z, Goldfine H, Klein EA. 2019. Caulobacter crescentus adapts to phosphate starvation by synthesizing anionic glycoglycerolipids and a novel glycosphingolipid. mBio 10:e00107-19. https://doi.org/10.1128/mBio.00107-19.
28. Jasim R, Han M-L, Zhu Y, Hu X, Hussein MH, Lin Y-W, Zhou QT, Dong CYD, Li J, Velkov T. 2018. Lipidomic analysis of the outer membrane vesicles from paired polymyxin-susceptible and -resistant Klebsiella pneumoniae clinical isolates. Int J Mol Sci 19:2356. https://doi.org/10.3390/ijms19082356.
29. Zhang Y, Li J, Wang J, Wang G. 2019. Pedobacter paludis sp. nov., isolated from wetland soil. Arch Microbiol 201:349–355. https://doi.org/10.1007/s00203-018-1605-0.
30. Harrison PJ, Dunn TM, Campopiano DJ. 2018. Sphingolipid biosynthesis in man and microbes. Nat Prod Rep 35:921–954. https://doi.org/10.1039/c8np00019k.
31. Hannun YA, Obeid LM. 2018. Sphingolipids and their metabolism in physiology and disease. Nat Rev Mol Cell Biol 19:175–191. https://doi.org/10.1038/nrm.2017.107.
32. Chung RWS, Kamili A, Tandy S, Weir JM, Gaire R, Wong G, Meikle PJ, Cohn JS, Rye K-A. 2013. Dietary sphingomyelin lowers hepatic lipid levels and inhibits intestinal cholesterol absorption in high-fat-fed mice. PLoS One 8:e55949. https://doi.org/10.1371/journal.pone.0055949.
33. Raichur S, Wang ST, Chan PW, Li Y, Ching J, Chaurasia B, Chaurasia B, Dogra S, Öhman MK, Takeda K, Sugii S, Pewzner-Jung Y, Futerman AH, Summers SA. 2014. CerS2 haploinsufficiency inhibits β-oxidation and confers susceptibility to diet-induced steatohepatitis and insulin resistance. Cell Metab 20:687–695. https://doi.org/10.1016/j.cmet.2014.09.015.
34. Turpin SM, Nicholls HT, Willmes DM, Mourier A, Brodesser S, Wunderlich CM, Mauer J, Xu E, Hammerschmidt P, Brönneke HS, Trifunovic A, LoSasso G, Wunderlich FT, Kornfeld J-W, Blüher M, Krönke M, Brüning JC. 2014. Obesity-induced CerS6-dependent C16:0 ceramide production promotes weight gain and glucose intolerance. Cell Metab 20:678–686. https://doi.org/10.1016/j.cmet.2014.08.002.
35. Brown EM, Ke X, Hitchcock D, Jeanfavre S, Avila-Pacheco J, Nakata T, Arthur TD, Fornelos N, Heim C, Franzosa EA, Watson N, Huttenhower C, Haiser HJ, Dillow G, Graham DB, Finlay BB, Kostic AD, Porter JA, Vlamakis H, Clish CB, Xavier RJ. 2019. Bacteroides-derived sphingolipids are critical for maintaining intestinal homeostasis and symbiosis. Cell Host Microbe 25:668–680.e7. https://doi.org/10.1016/j.chom.2019.04.002.
36. Lee-Sarwar K, Kelly RS, Lasky-Su J, Moody DB, Mola AR, Cheng T-Y, Comstock LE, Zeiger RS, O'Connor GT, Sandel MT, Bacharier LB, Beigelman A, Laranjo N, Gold DR, Bunyavanich S, Savage JH, Weiss ST, Brennan PJ, Litonjua AA. 2018. Intestinal microbial-derived sphingolipids are inversely associated with childhood food allergy. J Allergy Clin Immunol 142:335–338.e9. https://doi.org/10.1016/j.jaci.2018.04.016.
37. An D, Na C, Bielawski J, Hannun YA, Kasper DL. 2011. Membrane sphingolipids as essential molecular signals for Bacteroides survival in the intestine. Proc Natl Acad Sci U S A 108 Suppl 1:4666–4671. https://doi.org/10.1073/pnas.1001501107.
38. An D, Oh SF, Olszak T, Neves JF, Avci FY, Erturk-Hasdemir D, Lu X, Zeissig S, Blumberg RS, Kasper DL. 2014. Sphingolipids from a symbiotic microbe regulate homeostasis of host intestinal natural killer T cells. Cell 156:123–133. https://doi.org/10.1016/j.cell.2013.11.042.
39. Moye ZD, Valiuskyte K, Dewhirst FE, Nichols FC, Davey ME. 2016. Synthesis of sphingolipids impacts survival of Porphyromonas gingivalis and the presentation of surface polysaccharides. Front Microbiol 7:1919.
40. Rocha FG, Moye ZD, Ottenberg G, Tang P, Campopiano DJ, Gibson FC, III, Davey ME. 2020. Porphyromonas gingivalis sphingolipid synthesis limits the host inflammatory response. J Dent Res 99:568–576. https://doi.org/10.1177/0022034520908784.
41. Kato M, Muto Y, Tanaka-Bandoh K, Watanabe K, Ueno K. 1995. Sphingolipid composition in Bacteroides species. Anaerobe 1:135–139. https://doi.org/10.1006/anae.1995.1009.
42. von Gerichten J, Lamprecht D, Opálka L, Soulard D, Marsching C, Pilz R, Sencio V, Herzer S, Galy B, Nordström V, Hopf C, Gröne H-J, Trottein F, Sandhoff R. 2019. Bacterial immunogenic α-galactosylceramide identified in the murine large intestine: dependency on diet and inflammation. J Lipid Res 60:1892–1904. https://doi.org/10.1194/jlr.RA119000236.
43. Wieland Brown LC, Penaranda C, Kashyap PC, Williams BB, Clardy J, Kronenberg M, Sonnenburg JL, Comstock LE, Bluestone JA, Fischbach MA. 2013. Production of α-galactosylceramide by a prominent member of the human gut microbiota. PLoS Biol 11:e1001610. https://doi.org/10.1371/journal.pbio.1001610.
44. Haurat MF, Aduse-Opoku J, Rangarajan M, Dorobantu L, Gray MR, Curtis MA, Feldman MF. 2011. Selective sorting of cargo proteins into bacterial membrane vesicles. J Biol Chem 286:1269–1276. https://doi.org/10.1074/jbc.M110.185744.
45. Fahy E, Sud M, Cotter D, Subramaniam S. 2007. LIPID MAPS online tools for lipid research. Nucleic Acids Res 35:W606–W612. https://doi.org/10.1093/nar/gkm324.
46. Fahy E, Subramaniam S, Murphy RC, Nishijima M, Raetz CRH, Shimizu T, Spener F, van Meer G, Wakelam MJO, Dennis EA. 2009. Update of the LIPID MAPS comprehensive classification system for lipids. J Lipid Res 50 Suppl:S9–S14. https://doi.org/10.1194/jlr.R800095-JLR200.
47. Fahy E, Alvarez-Jarreta J, Brasher CJ, Nguyen A, Hawksworth JI, Rodrigues P, Meckelmann S, Allen SM, O'Donnell VB. 2019. LipidFinder on LIPID MAPS: peak filtering, MS searching and statistical analysis for lipidomics. Bioinformatics 35:685–687. https://doi.org/10.1093/bioinformatics/bty679.
48. Lynch A, Crowley E, Casey E, Cano R, Shanahan R, McGlacken G, Marchesi JR, Clarke DJ. 2017. The Bacteroidales produce an N-acylated derivative of glycine with both cholesterol-solubilising and hemolytic activity. Sci Rep 7:13270. https://doi.org/10.1038/s41598-017-13774-6.
49. Sohlenkamp C, Geiger O. 2016. Bacterial membrane lipids: diversity in structures and pathways. FEMS Microbiol Rev 40:133–159. https://doi.org/10.1093/femsre/fuv008.

50. Cohen LJ, Kang H-S, Chu J, Huang Y-H, Gordon EA, Reddy BVB, Ternei MA, Craig JW, Brady SF. 2015. Functional metagenomic discovery of bacterial effectors in the human microbiome and isolation of commendamide, a GPCR G2A/132 agonist. Proc Natl Acad Sci U S A 112:E4825–E4834. https://doi.org/10.1073/pnas.1508737112.
51. Olsen I, Nichols FC. 2018. Are sphingolipids and serine dipeptide lipids underestimated virulence factors of Porphyromonas gingivalis? Infect Immun 86:e00035-18. https://doi.org/10.1128/IAI.00035-18.
52. Clark RB, Cervantes JL, Maciejewski MW, Farrokhi V, Nemati R, Yao X, Anstadt E, Fujiwara M, Wright KT, Riddle C, La Vake CJ, Salazar JC, Finegold S, Nichols FC. 2013. Serine lipids of Porphyromonas gingivalis are human and mouse Toll-like receptor 2 ligands. Infect Immun 81:3479–3489. https://doi.org/10.1128/IAI.00803-13.
53. Nichols FC, Clark RB, Liu Y, Provatas AA, Dietz CJ, Zhu Q, Wang Y-H, Smith MB. 2020. Glycine lipids of Porphyromonas gingivalis are agonists for Toll-like receptor 2. Infect Immun 88:e00877-19. https://doi.org/10.1128/IAI.00877-19.
54. Kawai Y, Yano I, Kaneda K. 1988. Various kinds of lipoamino acids including a novel serine-containing lipid in an opportunistic pathogen Flavobacterium: their structures and biological activities on erythrocytes. Eur J Biochem 171:73–80. https://doi.org/10.1111/j.1432-1033.1988.tb13760.x.
55. Lynch A, Tammireddy SR, Doherty MK, Whitfield PD, Clarke DJ. 2019. The glycine lipids of Bacteroides thetaiotaomicron are important for fitness during growth in vivo and in vitro. Appl Environ Microbiol 85:e02157-18. https://doi.org/10.1128/AEM.02157-18.
56. Panevska A, Skočaj M, Križaj I, Maček P, Sepčić K. 2019. Ceramide phosphoethanolamine, an enigmatic cellular membrane sphingolipid. Biochim Biophys Acta Biomembr 1861:1284–1292. https://doi.org/10.1016/j.bbamem.2019.05.001.
57. Koropatkin NM, Martens EC, Gordon JI, Smith TJ. 2008. Starch catabolism by a prominent human gut symbiont is directed by the recognition of amylose helices. Structure 16:1105–1115. https://doi.org/10.1016/j.str.2008.03.017.
58. Zimmermann L, Stephens A, Nam S-Z, Rau D, Kübler J, Lozajic M, Gabler F, Söding J, Lupas AN, Alva V. 2018. A completely reimplemented MPI Bioinformatics Toolkit with a new HHpred server at its core. J Mol Biol 430:2237–2243. https://doi.org/10.1016/j.jmb.2017.12.007.
59. Schäffer AA, Aravind L, Madden TL, Shavirin S, Spouge JL, Wolf YI, Koonin EV, Altschul SF. 2001. Improving the accuracy of PSI-BLAST protein database searches with composition-based statistics and other refinements. Nucleic Acids Res 29:2994–3005. https://doi.org/10.1093/nar/29.14.2994.
60. Kelley LA, Mezulis S, Yates CM, Wass MN, Sternberg MJ. 2015. The Phyre2 Web portal for protein modeling, prediction and analysis. Nat Protoc 10:845–858. https://doi.org/10.1038/nprot.2015.053.
61. Deranieh RM, He Q, Caruso JA, Greenberg ML. 2013. Phosphorylation regulates myo-inositol-3-phosphate synthase: a novel regulatory mechanism of inositol biosynthesis. J Biol Chem 288:26822–26833. https://doi.org/10.1074/jbc.M113.479121.
62. Bachhawat N, Mande SC. 1999. Identification of the INO1 gene of Mycobacterium tuberculosis H37Rv reveals a novel class of inositol-1-phosphate synthase enzyme. J Mol Biol 291:531–536. https://doi.org/10.1006/jmbi.1999.2980.
63. Lu YH, Guan Z, Zhao J, Raetz CR. 2011. Three phosphatidylglycerol-phosphate phosphatases in the inner membrane of Escherichia coli. J Biol Chem 286:5506–5518. https://doi.org/10.1074/jbc.M110.199265.
64. Adams MM, Allison GE, Verma NK. 2001. Type IV O antigen modification genes in the genome of Shigella flexneri NCTC 8296. Microbiology (Reading) 147:851–860. https://doi.org/10.1099/00221287-147-4-851.
65. Nair A, Korres H, Verma NK. 2011. Topological characterisation and identification of critical domains within glucosyltransferase IV (GtrIV) of Shigella flexneri. BMC Biochem 12:67. https://doi.org/10.1186/1471-2091-12-67.
66. Kolly GS, Mukherjee R, Kilacsková E, Abriata LA, Raccaud M, Blaško J, Sala C, Dal Peraro M, Mikušová K, Cole ST. 2015. GtrA protein Rv3789 is required for arabinosylation of arabinogalactan in Mycobacterium tuberculosis. J Bacteriol 197:3686–3697. https://doi.org/10.1128/JB.00628-15.
67. Jackson M, Crick DC, Brennan PJ. 2000. Phosphatidylinositol is an essential phospholipid of mycobacteria. J Biol Chem 275:30092–30099. https://doi.org/10.1074/jbc.M004658200.
68. Reggiori F, Conzelmann A. 1998. Biosynthesis of inositol phosphoceramides and remodeling of glycosylphosphatidylinositol anchors in Saccharomyces cerevisiae are mediated by different enzymes. J Biol Chem 273:30550–30559. https://doi.org/10.1074/jbc.273.46.30550.
69. Cerbón J, Falcon A, Hernández-Luna C, Segura-Cobos D. 2005. Inositol phosphoceramide synthase is a regulator of intracellular levels of diacylglycerol and ceramide during the G1 to S transition in Saccharomyces cerevisiae. Biochem J 388:169–176. https://doi.org/10.1042/BJ20040475.
70. Wang Y-H, Nemati R, Anstadt E, Liu Y, Son Y, Zhu Q, Yao X, Clark RB, Rowe DW, Nichols FC. 2015. Serine dipeptide lipids of Porphyromonas gingivalis inhibit osteoblast differentiation: relationship to Toll-like receptor 2. Bone 81:654–661. https://doi.org/10.1016/j.bone.2015.09.008.
71. Nemati R, Dietz C, Anstadt EJ, Cervantes J, Liu Y, Dewhirst FE, Clark RB, Finegold S, Gallagher JJ, Smith MB, Yao X, Nichols FC. 2017. Deposition and hydrolysis of serine dipeptide lipids of Bacteroidetes bacteria in human arteries: relationship to atherosclerosis. J Lipid Res 58:1999–2007. https://doi.org/10.1194/jlr.M077792.
72. Whitaker WR, Shepherd ES, Sonnenburg JL. 2017. Tunable expression tools enable single-cell strain distinction in the gut microbiome. Cell 169:538–546.e12. https://doi.org/10.1016/j.cell.2017.03.041.
73. Huang JY, Lee SM, Mazmanian SK. 2011. The human commensal Bacteroides fragilis binds intestinal mucin. Anaerobe 17:137–141. https://doi.org/10.1016/j.anaerobe.2011.05.017.
74. Donaldson GP, Chou W-C, Manson AL, Rogov P, Abeel T, Bochicchio J, Ciulla D, Melnikov A, Ernst PB, Chu H, Giannoukos G, Earl AM, Mazmanian SK. 2020. Spatially distinct physiology of Bacteroides fragilis within the proximal colon of gnotobiotic mice. Nat Microbiol 5:746–756. https://doi.org/10.1038/s41564-020-0683-3.
75. Lee SM, Donaldson GP, Mikulski Z, Boyajian S, Ley K, Mazmanian SK. 2013. Bacterial colonization factors control specificity and stability of the gut microbiota. Nature 501:426–429. https://doi.org/10.1038/nature12447.
76. Donaldson GP, Ladinsky MS, Yu KB, Sanders JG, Yoo BB, Chou W-C, Conner ME, Earl AM, Knight R, Bjorkman PJ, Mazmanian SK. 2018. Gut microbiota utilize immunoglobulin A for mucosal colonization. Science 360:795–800. https://doi.org/10.1126/science.aaq0926.
77. Johnson EL, Heaver SL, Waters JL, Kim BI, Bretin A, Goodman AL, Gewirtz AT, Worgall TS, Ley RE. 2020. Sphingolipids produced by gut bacteria enter host metabolic pathways impacting ceramide levels. Nat Commun 11:2471. https://doi.org/10.1038/s41467-020-16274-w.
78. Rocha FG, Ottenberg G, Eure ZG, Davey ME, Gibson FC. 2021. Sphingolipid-containing outer membrane vesicles serve as a delivery vehicle to limit macrophage immune response to Porphyromonas gingivalis. Infect Immun 89:e00614-20. https://doi.org/10.1128/IAI.00614-20.
79. Jones EJ, Booth C, Fonseca S, Parker A, Cross K, Miquel-Clopés A, Hautefort I, Mayer U, Wileman T, Stentz R, Carding SR. 2020. The uptake, trafficking, and biodistribution of Bacteroides thetaiotaomicron generated outer membrane vesicles. Front Microbiol 11:57.
80. Bligh EG, Dyer WJ. 1959. A rapid method of total lipid extraction and purification. Can J Biochem Physiol 37:911–917. https://doi.org/10.1139/o59-099.
81. Hsu F-F, Turk J, Zhang K, Beverley SM. 2007. Characterization of inositol phosphorylceramides from Leishmania major by tandem mass spectrometry with electrospray ionization. J Am Soc Mass Spectrom 18:1591–1604. https://doi.org/10.1016/j.jasms.2007.05.017.
82. Hsu FF. 2016. Complete structural characterization of ceramides as $[M-H]^-$ ions by multiple-stage linear ion trap mass spectrometry. Biochimie 130:63–75. https://doi.org/10.1016/j.biochi.2016.07.012.
83. Hsu FF, Turk J. 2009. Electrospray ionization with low-energy collisionally activated dissociation tandem mass spectrometry of glycerophospholipids: mechanisms of fragmentation and structural characterization. J Chromatogr B Analyt Technol Biomed Life Sci 877:2673–2695. https://doi.org/10.1016/j.jchromb.2009.02.033.
84. Sud M, Fahy E, Cotter D, Azam K, Vadivelu I, Burant C, Edison A, Fiehn O, Higashi R, Nair KS, Sumner S, Subramaniam S. 2016. Metabolomics Workbench: an international repository for metabolomics data and metadata, metabolite standards, protocols, tutorials and training, and analysis tools. Nucleic Acids Res 44:D463–D470. https://doi.org/10.1093/nar/gkv1042.